American Society of Hematology
2021 L Street NW, Suite 900,
Washington, DC 20036
Phone: 202-776-0544 | Fax 202-776-0545
editorial@hematology.org

Secreted Mutant Calreticulins As Rogue Cytokines in Myeloproliferative Neoplasms

Tracking no: BLD-2022-016846R2

Christian Pecquet (Ludwig Institute for Cancer Research Brussels, Belgium) Nicolas Papadopoulos (Ludwig Institute for Cancer Research, Belgium) Thomas Balligand (Ludwig Institute for Cancer Research Brussels, Belgium) Ilyas CHACHOUA (Université Catholique de Louvain, Belgium) Amandine Tisserand (INSERM, Unité Mixte de Recherche 1287, Institut Gustave Roussy, France) Gaëlle Vertenoeil (Ludwig Institute for Cancer Research Brussels, Belgium) Audrey Nedelec (Université catholique de Louvain and de Duve Institute, Belgium) Didier Vertommen (de Duve Institute,) Anita Roy (Ludwig Institute for Cancer Research Brussels,) Caroline Marty (INSERM UMR1287, Gustave Roussy, France) Harini Nivarthi (CeMM, Austria) Jean-Philippe Defour (Ludwig Institute for Cancer Research, Belgium) Mira El-Khoury (Gustave Roussy, France) Eva Hug (Myelopro Diagnostics and Research GmbH,) Erica Xu (Myelopro Diagnostics and Research GmbH,) Oleh Zagrijtschuk (Dr. med. Oleh Zagrijtschuk, MSc, Austria) Emmanuel Fertig (National Institute of Pathology Victor Babeș, Romania) Daciana Marta (National Institute of Pathology Victor Babeș, Romania) Heinz Gisslinger (Medical University of Vienna, Austria) Bettina Gisslinger (Medical University of Vienna, Austria) Martin Schalling (Medical University of Vienna, Austria) Ilaria Casetti (University of Pavia, Italy) Elisa Rumi (University of Pavia, Italy) Daniela Pietra (Fondazione IRCCS Policlinico San Matteo, Italy) Chiara Cavalloni (Fondazione IRCCS Policlinico San Matteo, Italy) Luca Arcaini (Division of Hematology, Fondazione IRCCS Policlinico San Matteo, Italy) Mario Cazzola (University of Pavia, Italy) Norio Komatsu (Juntendo University School of Medicine, Japan) Yoshihiko Kihara (Juntendo University School of Medicine, Japan) Yoshitaka Sunami (Juntendo university school of medicine, Japan) Yoko Edahiro (Juntendo University School of Medicine, Japan) Marito Araki (Juntendo University School of Medicine, Japan) Roman Lesyk (Danylo Halytsky Lviv National Medical University, Lviv, Ukraine, Ukraine) Veronika Buxhofer-Ausch (Johannes Kepler University Linz, Austria) Sonja Heibl (Klinikum Wels-Grieskirchen, Austria) Florence Pasquier (Institut Gustave Roussy, France) Violaine Havelange (Cliniques Universitaires Saint-Luc,) Isabelle Plo (INSERM UMR 1287, France) William Vainchenker (Gustave Roussy, France) Robert Kralovics (Université catholique de Louvain and de Duve Institute, Belgium) Stefan Constantinescu (Ludwig Institute for Cancer Research Brussels, Brussels, Belgium., Belgium)

Abstract:
Mutant calreticulin (CALR) proteins resulting from a -1/+2 frameshifting mutation of the *CALR* exon 9 carry a novel C-terminal amino-acid sequence and drive the development of myeloproliferative neoplasms (MPNs). Mutant CALRs were shown to interact with and activate the thrombopoietin receptor (TpoR/MPL) in the same cell. We report that mutant CALR proteins are secreted and can be found in patient plasma at levels up to 160 ng/ml, with a mean of 25.64 ng/ml. Plasma mutant CALR is found in complex with soluble Transferrin Receptor 1 (sTFRC) that acts as a carrier protein and increases CALR mutant half-life. Recombinant mutant CALR proteins bound and activated the TpoR on cell lines and primary megakaryocytic progenitors from *CALR*-mutated patients where they drive Tpo-independent colony formation. Importantly, the CALR-sTFRC complex remains functional for TpoR activation. By bioluminescence resonance energy transfer assay, we show that mutant CALR proteins produced in one cell can specifically interact *in trans* with the TpoR on a target cell. Cells that carry both TpoR and mutant CALR are hypersensitive to exogenous CALR mutant proteins in comparison to cells that only carry TpoR, and respond to levels of CALR mutant proteins similar to those in patient plasma. This is consistent with CALR mutated cells exposing at the cell-surface TpoR carrying immature N-linked sugars. Thus, secreted mutant CALR proteins will act more specifically on the MPN clone. In conclusion, a chaperone, CALR, can turn into a rogue cytokine through somatic mutation of its encoding gene.

Conflict of interest: COI declared - see note

COI notes: RK and SNC and are co-founders of MyeloPro GmbH.

Preprint server: No;

Author contributions and disclosures: CP, NP, TB, IC, AT planned paper strategy, performed experiments, interpreted data and wrote the paper; CP, AN, IC, GV, JPD planned and performed transcriptional experiments, CP performed functional murine cell lines and primary cell experiments, TB planned and performed BRET experiments, NP performed CALR mutant protein characterization from patient and primary mouse model plasmas, identify the TFRC-CALR interaction from plasma patients and performed characterization of the CALR-TFRC interaction, DV and NP performed mass spectrometry experiments and analyzed the data, EH , EX, OZ, RK performed study on patient plasma, EF and DSM performed immunoelectron microscopy, HG, BG, MS, IC, ER, DP, CC, LA, MC, NK, YK, YS, YE, MA, VBA, SH, VH selected patients, characterized allele burdens for MPN driver mutations and interpreted data on plasma levels of CALR mutants in the context of type of mutation, allele burden and MPN subtype. AT, MEK, CM performed megakaryocytic colonies from CALR-mutated patients and IP and VW supervised and analyzed these experiments. SNC, RK and WV planned research interpreted data and wrote the paper.

Non-author contributions and disclosures: No;

Agreement to Share Publication-Related Data and Data Sharing Statement: emails to the corresponding author

Clinical trial registration information (if any):

Secreted Mutant Calreticulins As Rogue Cytokines in Myeloproliferative Neoplasms

Christian Pecquet[1,2*], Nicolas Papadopoulos[1,2*], Thomas Balligand[1,2*], Ilyas Chachoua[1,2*], Amandine Tisserand[3-5,*], Gaëlle Vertenoeil[1,2], Audrey Nédélec[1,2], Didier Vertommen[2], Anita Roy[1,2], Caroline Marty[3,5-6], Harini Nivarthi[7], Jean-Philippe Defour[1,2], , Mira El-Khoury[3,5-6], Eva Hug[8], Erica Xu[8], Oleh Zagrijtschuk[9], Tudor E. Fertig[10], Daciana S. Marta[10], Heinz Gisslinger[11], Bettina Gisslinger[11], Martin Schalling[11], Ilaria Casetti[12], Elisa Rumi[12], Daniela Pietra[12], Chiara Cavalloni[12], Luca Arcaini[12], Mario Cazzola[12], Norio Komatsu[13], Yoshihiko Kihara[13], Yoshitaka Sunami[13], Yoko Edahiro[13], Marito Araki[14], Roman Lesyk[15,16], Veronika Buxhofer-Ausch[17,18], Sonja Heibl[19], Florence Pasquier[3-5,20], Violaine Havelange[2,21], Isabelle Plo[3,5-6], William Vainchenker[3,5-6], Robert Kralovics[22#] and Stefan N. Constantinescu[1,2,23,24#]

[1]Ludwig Institute for Cancer Research Brussels, Brussels, Belgium; [2]Université catholique de Louvain and de Duve Institute, Brussels, Belgium; [3]INSERM, Unité Mixte de Recherche 1287, Gustave Roussy, Villejuif, France, [4]Université Paris Cité, Unité Mixte de Recherche 1287, Institut Gustave Roussy, Villejuif, France; [5]Gustave Roussy, Unité Mixte de Recherche 1287, Villejuif, France, [6]Université Paris-Saclay, Unité Mixte de Recherche 1287, Institut Gustave Roussy, Villejuif, France;[7]CeMM Research Center for Molecular Medicine of the Austrian Academy of Sciences, Vienna, Austria, [8]MyeloPro Diagnostics and Research GmbH, Vienna, Austria, [9]Dr. Oleh Zagrijtschuk, Zieglergasse 55/2/4, 1070 Vienna, Austria, [10]Ultrastructural Pathology Lab and Bioimaging, Victor Babeș Institute of Pathology, Bucharest, Romania, [11]Department of Internal Medicine I, Division of Hematology and Blood Coagulation, Medical University of Vienna, Vienna, Austria, [12]Division of Hematology, Fondazione IRCCS Policlinico San Matteo and University of Pavia, Pavia, Italy, [13]Department of Hematology, Juntendo University Graduate School of Medicine, Japan, [14]Department of Transfusion Medicine and Stem Cell Regulation, Juntendo University Graduate School of Medicine, Japan, [15]Department of Biotechnology and Cell Biology, Medical College, University of Information Technology and Management in Rzeszow, Sucharskiego 2, 35-225 Rzeszow, Poland, [16] Department of Pharmaceutical, Organic and Bioorganic Chemistry, Danylo Halytsky Lviv National Medical University, Pekarska 69, 79010, Lviv-10, Ukraine, [17]Ordensklinikum Linz Elisabethinen, Department of Internal Medicine I with Hematology, Stem Cell Transplantation, Hemostaseology and Medical Oncology; Fadingerstrasse 1, 4020 Linz, Austria [18]Johannes Kepler University Linz, Medical Faculty, Altenberger Strasse 69, 4040 Linz, Austria, [19]Department of Internal Medicine IV, Klinikum Wels-Grieskirchen, Wels, Austria, [20]Department of Hematology, Institut Gustave Roussy, Villejuif, France, [21]Department of Hematology, Cliniques universitaires Saint-Luc, Brussels, Belgium, [22]Department of Laboratory Medicine, Medical University of Vienna, Vienna, Austria, [23]Walloon Excellence in Life Sciences and Biotechnology (WELBIO), Brussels, Belgium, [24]Ludwig Institute for Cancer Research, Nuffield Department of Medicine, Oxford University, Oxford, UK.

*co-first authors
[#]corresponding authors

Correspondence:

- Stefan N. Constantinescu, Ludwig Institute for Cancer Research Brussels. Avenue Hippocrate 74, UCL 75-4, Brussels B-1200, Belgium; e-mail: Stefan.constantinescu@bru.licr.org; Tel: 322-764-75-40.
- Robert Kralovics, Department of Laboratory Medicine, Medical University of Vienna, Anna Spiegel Research Building, Lazarettgasse 14, AKH BT25.2, Level 6, Vienna, Austria; e-mail: robert.kralovics@meduniwien.ac.at; Tel: 43-(0)1-40400-73510.

Key Points

1) Mutant CALR proteins are secreted to the plasma of MPN patients in complex with sTFRC, and can act as a rogue cytokine by activating the TpoR on neighboring cells.
2) TpoR-expressing cells with a *CALR* mutation are uniquely sensitive to the levels of circulating mutant CALR proteins seen in patients.

Abstract

Mutant calreticulin (CALR) proteins resulting from a -1/+2 frameshifting mutation of the *CALR* exon 9 carry a novel C-terminal amino-acid sequence and drive the development of myeloproliferative neoplasms (MPNs). Mutant CALRs were shown to interact with and activate the thrombopoietin receptor (TpoR/MPL) in the same cell. We report that mutant CALR proteins are secreted and can be found in patient plasma at levels up to 160ng/mL, with a mean of 25.64ng/mL. Plasma mutant CALR is found in complex with soluble Transferrin Receptor 1 (sTFRC) that acts as a carrier protein and increases CALR mutant half-life. Recombinant mutant CALR proteins bound and activated the TpoR on cell lines and primary megakaryocytic progenitors from *CALR*-mutated patients where they drive Tpo-independent colony formation. Importantly, the CALR-sTFRC complex remains functional for TpoR activation. By bioluminescence resonance energy transfer assay, we show that mutant CALR proteins produced in one cell can specifically interact *in trans* with the TpoR on a target cell. Cells that carry both TpoR and mutant CALR are hypersensitive to exogenous CALR mutant proteins in comparison to cells that only carry TpoR, and respond to levels of CALR mutant proteins similar to those in patient plasma. This is consistent with CALR mutated cells exposing at the cell-surface TpoR carrying immature N-linked sugars. Thus, secreted mutant CALR proteins will act more specifically on the MPN clone. In conclusion, a chaperone, CALR, can turn into a rogue cytokine through somatic mutation of its encoding gene.

Introduction

Frameshifting (-1/+2) mutations in the exon 9 of the calreticulin (*CALR)* gene are responsible for 20-30% cases of essential thrombocythemia (ET) and primary myelofibrosis (PMF)[1,2]. Belonging to the *BCR-ABL* negative myeloproliferative neoplasms (MPNs), ET and PMF are clonal malignancies of the hematopoietic system. The two major prevalent exon 9 frameshifting mutations of *CALR* are a 52 base-pair deletion (type-1: del52, c.1092_1143del) and a 5 base-pair insertion (type-2: ins5, c.1154_1155insTTGTC)[1,2]. The oncogenic mutant CALR protein has been shown to always result from a -1/+2 frameshifting mutation in the exon 9 of the *CALR* gene. This leads to a novel mutant C-terminal end-tail that is rich in positively charged and hydrophobic residues, unlike the wild-type CALR [3] and loses the endoplasmic reticulum (ER)-retention KDEL signal peptide.

We and others have shown that the mutant end-tail of CALR enables the specific pathological activation of the thrombopoietin receptor (TpoR)[4-10], which via the JAK-STAT pathway drives the proliferation of hematopoietic cells. Mutant CALR and TpoR complexes traffic through the secretory pathway to the cell surface[11,12]. CALR mutants require oligomerization in order to activate TpoR[12,13] and the first N-glycosylation site of TpoR at residue Asn117 to be present for oncogenic activation[4]. Asn117 remains immature *N*-glycosylated at the cell surface due to CALR mutants shielding it from processing in the Golgi apparatus[12]. CALR mutants were reported by others and us to be circulating in the peripheral blood of patients suffering from *CALR* mutated MPNs or engineered mice[14-17]. Wild-type CALR may also go to the cell surface under specific conditions[11,18-21], or be secreted by macrophages to enhance phagocytosis of cancer cells[22].

Here we asked whether secreted mutant CALRs may act in a paracrine and/or autocrine fashion to activate the TpoR of adjacent cells and if this ‘rogue cytokine’ effect would be relevant to MPN pathogenesis.

Main Methods

ELISA

ELISA plates were coated with a polyclonal rabbit antibody (SAT602) or a monoclonal rat antibody (clone 11) that recognize a peptide derived from the mutant CALR C-terminal sequence. After blocking (5% BSA + 0.05% Tween-20 in PBS), plates were probed with plasma samples diluted in blocking buffer. Purified mutant-CALR protein produced in Expi-293F cells (Thermo Fisher Scientific, Merelbeke, Belgium) was included as standard for quantification. For detection, an anti-CALR antibody (FMC75, Abcam, Cambridge, UK) in combination with an anti-mouse IgG-HRP antibody (Southern Biotech, Birmingham, AL) was used and TMB (3,3',5,5'-Tetramethylbenzidine, Thermo Fisher Scientific) was added as substrate. Absorbance was measured with a microplate reader (SpectraMax i3, Molecular Devices, Silicon Valley, CA) at 450 and 620nm. For measuring stability of recombinant human (rh) CALR del52, we incubated rhCALR del52 in either indicated medium or plasma from healthy individual for several periods at 37°C and then measured levels by ELISA and detection with a chicken monoclonal antibody raised against the C-terminal mutated tail in combination with an anti-chicken IgG-HRP antibody (Abcam, Cambridge, UK).

Transcriptional Assays

Dual luciferase assay was performed as described before [4].

Immunoelectron microscopy

Cells were fixed using 4% paraformaldehyde, 0.5% glutaraldehyde and 1.4% sucrose (pH 7.4), then embedded in London Resin White (LR White) by manufacturer protocols (Agar Scientific, UK). Sections were labeled on-grid with a primary antibody, then a gold-conjugated secondary at 1:250 dilution (gold size 0.8, 6 or 10 nm, Aurion, The Netherlands). Primary antibody was omitted for negative controls. Blocking was done with bovine serum albumin (0.2%) and a solution for goat antibodies (Aurion, The Netherlands). Micrographs were recorded using the 4k×4k Ceta camera of a Talos 200C transmission electron microscope (ThermoFisher Scientific), at 22000x to 36000x nominal magnification.

Confocal microscopy

HEK293T were plated on Ibidiμ-slide and transfected with TFRC-mCherry and CALR-linker-GFP fusion proteins 48h before imaging. Live cells were examined with a confocal server spinning disc Zeiss platform equipped with a x100 objective.

Megakaryocyte colony forming unit assay using human samples

$CD34^+$ cells were purified from patient peripheral blood and cultured for 3 days in serum-free medium in presence of Tpo (20ng/mL) (Kirin Brewery, Tokyo, Japan) and SCF (25ng/mL) (Biovitrum AB, Stockholm, Sweden). $CD34^+CD41^+$ progenitors were sorted using anti-CD34-FITC, anti-CD41-PE and were cloned at 1 cell/well in 96 wells plate in serum-free medium without cytokine, with SCF only, with SCF + Tpo (20ng/mL), with SCF ± rhCALR WT or SCF ± rhCALR del52. Megakaryocyte (MK) colonies were counted at day 5.

Proliferation assay (Celltiter-Glo assay)

Proliferation assays were performed as described [4].

NanoBRET assay and conditioned medium preparation

NanoBRET experiments were performed as described [12].

Results

CALR mutant proteins are detectable in the plasma of MPN patients and correlate with the status of disease

A total of 159 plasma samples from patients were analyzed by ELISA for presence of circulating mutant CALR proteins using a specific antibody that does not recognize non-mutated CALR (111 *CALR* mutated, 35 *JAK2*-V617F positive, 2 triple-negative and 11 healthy controls). Soluble mutant CALR was detectable in 106 out of 111 *CALR* mutated patients with a mean level of 25.64ng/mL. No signal was detected for *JAK2*-V617F positive, triple negative patients or healthy controls (**Figure 1A**). The most represented CALR mutation was type1-del52 (64 patients), followed by type2-ins5 (33 patients). 14 less common mutations were also observed (1 patient for each variant). Grouping all the mutations in type1-like, type2-like and other mutations did not reveal any significant difference in the amount of soluble mutant CALR among the first two groups, but was significantly lower in patients carrying other types of mutations (**Figure 1B**). Interestingly, 4 out of 5 samples with non-detectable mutant CALR belong to patients carrying uncommon mutation types, del22, del1, type28, type34, as defined in [2]. Mutational CALR burden and clinical diagnosis data were available for 57 patients. From those, plasma levels of soluble mutant CALR were directly correlated to the allele burdens in the blood (**Figure 1C**). We observed that mutant soluble CALR levels were significantly higher in patients with a diagnosis of PMF and pre-PMF when compared to patients with a diagnosis of ET (**Figure 1D**).

Immunoelectron microscopy detects mutant CALR proteins in Golgi apparatus and secretory vesicles

The results above suggested that mutant CALRs are secreted by the MPN clone. While we established the presence of mutant CALR in the secretory pathway of cells that also express TpoR [12] we asked whether CALR mutants are localized in the secretory pathway also in cells that only express CALR mutants, like myeloid or lymphoid cells of the mutated *CALR* clone. To this end we used transmission electron microscopy firstly on pro-B BaF3 cells expressing either CALR del52 or CALR WT tagged with a Flag sequence at the C-terminus in the absence of TpoR. Immunoelectron microscopy with anti-Flag and gold-conjugated secondary antibody

showed that CALR-del52 localized in both the *cis*-Golgi and *trans*-Golgi compartments, as well as in various vesicles distributed between the *trans*-Golgi network and the plasma membrane (**Figure 2A**). CALR WT was mostly localized in the ER and to a lower extent in the nucleus with very low levels in the *cis*- or *trans*-Golgi (**Figure 2B**).

We then turned to CRISPR-modified BaF3 TpoR *Calr*^{mut} cells that express endogenous level of CALR mutant (described previously [10]). Using an anti-N terminus CALR antibody we noted plasma membrane labelling (**Figure 2C**), suggesting that secretion of CALR mutant is maintained in this cell line. In contrast, in control CRISPR cells, endogenous WT CALR localized mostly in the ER and perinuclear space, nucleus, and weakly in the Golgi (G) network (**Figure 2D**). Similar differences were observed in primary bone marrow cells from *Calr*$^{del52/WT}$ KI mice and *Calr*$^{WT/WT}$ controls with an anti-N-terminus antibody (**Figure 2E and F**). Finally, we confirmed these data using a mutant CALR specific antibody, SAT602 which detects the C-terminus of the mutant CALR del52. The antibody also demonstrated labelling of plasma membrane and vesicles between *trans*-Golgi network and plasma membrane, as well as ectosomes, in the BaF3 TpoR *Calr*^{mut} cell line (**Figure 2G and H**) and primary bone marrow cells from *Calr* $^{del52/WT}$ KI mice (**Figure 2I**).

We next tested *in vivo* whether secretion occurs only from TpoR cells or also from other cells of the clone. We used *Calr*$^{del52/WT}$ KI mice that had been crossed with *Mpl*-/- mice. Remarkably, while intracellular CALR del52 was strongly reduced in absence of TpoR, it was still highly present in the plasma in mice lacking TpoR (**Figure 3A**). The high proportion of plasma CALR del52 in *MPL* -/- mice despite low intracellular expression suggested that cells that do not express TpoR are more able to secrete it. Consistently, comparison of secretion levels in cells co-transfected with CALR del52 and either TpoR or an empty vector revealed that the lack of TpoR resulted in enhanced secretion of CALR del52 (**Supplementary Figure 1A**). Flow-cytometry analysis showed that cell surface CALR del52 was also increased in absence of TpoR (**Supplemental Figure 1B**). Together, this suggests that the main source of plasma CALR mutant comes from cells of the clone that do not express TpoR.

Plasma soluble Transferrin Receptor 1 is a carrier protein for CALR mutant

To study the functional relevance of extracellular CALR mutant, we produced recombinant human CALR del52 (rhCALR del52) and CALR WT (rhCALR WT)

(**Supplementary Figure 2A-B**) and validated its correct folding by thermal shift (**Supplementary Figure 2C**). We assessed the stability of rhCALR del52 by measuring its half-life in culture medium (without serum supplementation) after incubation at 37°C and detection by ELISA. Analysis revealed a half-life of 30.72 minutes (**Figure 3B**). Strikingly, the stability of plasma CALR mutant was over 10 times higher with an average half-life of 426.3 min (**Figure 3C**) and immunoprecipitation followed by western blotting confirmed that CALR proteins were intact (**Figure 3D**, left panel) and quantification validated the levels detected by ELISA (**Figure 3D**, right panel). To assess whether CALR mutant could be stabilized by other proteins in plasma, we immunoprecipitated the plasma from 5 patients and 5 healthy controls with a mutant C-terminus specific antibody (**Figure 4A-B**) and analyzed the co-precipitating proteins by mass spectrometry. The plasma soluble Transferrin Receptor 1 (sTFRC) was the only protein detected in large quantities in 5 out of 5 patients and not in control samples (**Figure 4C and Supplementary File 1**). The presence of the sTFRC-CALR mutant complex in the plasma of 4 additional patients was confirmed by western-blotting with anti-TFRC antibody after immunoprecipitation of CALR mutant (**Supplementary Figure 3A**). To estimate the fraction of plasma CALR mutant in complex with sTFRC, we quantified by western blotting the amount of sTFRC that co-immunoprecipitated with plasma CALR from 4 other patients. By also measuring the amount of plasma mutant CALR in the immunoprecipitation product, we could approximate the fraction of plasma CALR in complex with sTFRC to an average of ~60% for these 4 patients given a 1:1 molar ratio (**Supplementary Figure 3B-D**).

These results suggested that sTFRC may act that as a carrier protein of plasma CALR mutant and increase its half-life. We measured the stability of rhCALR del52 in culture medium with 10% Fetal Bovine Serum supplemented or not with 2µg/mL or 4µg/mL of sTFRC. Addition of serum resulted in higher half-life (73.38 min.) and gradual increase in stability was observed with 2µg/mL (113.3 min) and 4µg/mL (143.2 min) of sTFRC, in the range of normal sTFRC plasma concentration (~5µg/mL[23]) (**Figure 4D**). Interestingly, like TpoR, TFRC is a highly N-glycosylated protein. This led us to hypothesize that interaction between CALR mutant and TFRC could already occur in the secretory pathway. We used confocal microscopy to assess intracellular colocalization between TFRC-mCherry and CALR-GFP fusion proteins in living cells. CALR WT exhibited an ER-like localization without significant

colocalization with TFRC while CALR del52 was mostly present in intracellular vesicles and strongly colocalized with TFRC (**Figure 4E**). By mass spectrometry, we found that like TpoR[12], TFRC retained a high proportion of high-mannose immature N-glycans on Asn251 in cells expressing CALR del52 (**Figure 4F**). Remarkably, this differential N-glycosylation was only detected in the cleaved fragment of TFRC that is secreted, hinting that CALR del52 may favor its cleavage, as also suggested by the increased cleaved fraction in CALR del52 expressing cells (**Figure 4F**). We concluded that stabilization of the complex is favored by the N-glycans interactions formed intracellularly and that adding mutant CALR to plasma will not recover all interactions, as the recombinant sTFRC possesses fewer immature sugars than the one secreted with CALR mutant[24]**.** This explains why adding CALR del52 to healthy subject plasma only very modestly increases half-life from 30 min to 45 min (**Supplemental Figure 2D**).

CALR mutant proteins initiate proliferation of BaF3 expressing TpoR and mutant CALR in a rogue cytokine fashion

To probe the ability of soluble CALR to induce cytokine-independent proliferation of BaF3 cells, we first defined the amount of recombinant CALR that best mimicked plasma levels of CALR mutant found in patient plasma. We referred to basic pharmacokinetic equations to derive the single dose concentration that would best mimic a steady state concentration average similar to what is observed *in vivo*. The average plasma concentration (C_p) is given by [25]:

$$(1) \qquad C_p = \frac{1}{0.693} * F * D * t_{\frac{1}{2}} * \frac{1}{\tau}$$

Where F is the bioavailability, D is the dose, $t_{\frac{1}{2}}$ is the half-life and τ the dose interval.

The bioavailability was assumed to be maximum *in vitro* so that F =1, half-life was determined experimentally in culture medium with 10% FBS (**Figure 4D**) and dose interval was set at $\tau = 24\mathrm{h}$. Supplemental Table 1 gives the relationship between single-dose treatment and corresponding average concentration (C_p) over the experimental timeframe. In comparison, recombinant truncated human Tpo (rhTpo) used in *in vitro* assays is similar to that described in [26] with a half-life of 1.56h. A single dose of rhTpo of 10ng/mL over 24h thus has a C_p of 0.94ng/mL, slightly above the range of plasma Tpo detected in healthy control (0.108-0.506ng/mL) [27].

Based on the above results, we used several concentrations of CALR del52 from 0.01 µg/mL (C_p=0.73ng/mL) to 100 µg/mL (C_p=7.3µg/mL) with a dosing interval of 24h. Using this approach, we measured proliferation of BaF3 cells at 72h. Remarkably, we could detect a significant increase already at 0.01 µg/mL (C_p=0.73ng/mL) and a dose-dependent increase up to 100 µg/mL (C_p=7.3µg/mL) (**Figure 5A**) in BaF3 TpoR *Calr*$^{mut\ 10}$ but not in BaF3 parental or BaF3 TpoR *Calr*^{wt} that do not express mutant CALR. Cells that co-express TpoR and a CALR mutant are thus hyper-sensitive to exogenous mutant CALR proteins compared to cells that only express wild-type endogenous CALR. In comparison, addition of 10ng/mL of Tpo resulted in increased proliferation similar to that induced by an average concentration of C_p=73ng/mL, in the range of the what was found in patients' plasma (**Figure 5B**). EC50 was estimated to ~100ng/mL of rhCALR del52 on the growth of BaF3 TpoR *Calr*^{mut}, in the range of plasma concentration found in patients. In comparison, Tpo EC50 was of 0.62ng/mL and 2.02ng/mL in BaF3 TpoR *Calr*^{wt} and BaF3 TpoR *Calr*^{mut}, respectively. Remarkably, maximum response was higher with exogeneous CALR del52 than with Tpo for BaF3 TpoR *Calr*^{mut} cells, indicating that the latter respond better to plasma CALR mutant than to Tpo (**Supplementary Figure 4**). The ability of rhCALR del52 to induce proliferation BaF3 TpoR *Calr*^{mut} was further confirmed by thymidine incorporation experiment (**Supplementary Figure 5A**).

Low levels of soluble CALR mutants are able to induce JAK-STAT signaling by selectively activating TpoR at the cell surface of *Calr* mutated cells

To measure specifically the activation of the JAK-STAT pathway, we transfected the Spi-Luc luciferase STAT5 reporter [28] in BaF3 TpoR *Calr*^{mut}, BaF3 TpoR *Calr*^{wt} or parental BaF3 cells and measured STAT5 activation 24h after stimulation with rhCALR del52. In BaF3 TpoR *Calr*^{mut} cells we could detect a dose-dependent STAT5 activation by rhCALR del52 starting at 0.1µg/mL (C_p=7.3ng/mL) (2-fold) and a plateau (4-fold) achieved at 1µg/mL (C_p=73ng/mL), as compared to vehicle (**Figure 5C**). Like for growth assay, the activity induced by 1µg/mL (C_p=73ng/mL) of rhCALR del52 was comparable to stimulation by 10ng/mL of Tpo (C_p=0.94ng/mL).

In sharp contrast, BaF3 TpoR *Calr*^{wt} required a considerably higher concentration of rhCALR del52 (100µg/mL, C_p=7.3µg/mL) in order to detect a 2.5-fold increased

STAT5 activation, thus a 1,000-fold difference in sensitivity (**Supplementary Figure 5B)** and parental BaF3 cells were not stimulated by rhCALR del52 (**Supplementary Figure 5C)**. Surprisingly, we could detect a 1.5 to 2-fold increased STAT5 activation upon stimulation of BaF3 TpoR *Calr*^{mut} cells with 10 to 100µg/mL of rhCALR WT respectively, thus a 100- to 1,000-fold difference when compared to rhCALR del52 (**Figure 5C**). CALR WT might be interacting with surface bound TpoR-CALR mutant complexes and stabilizing them, possibly pointing to a potential low intrinsic affinity of CALR globular domain to TpoR.

We then verified that TFRC did not prevent CALR mutant mediated activation of TpoR. Since interaction of CALR mutant with TFRC relies at least partially on interaction with immature N-glycans (**Figure 4F**), we first used the approach of over-expressing TFRC intracellularly. Over-expression of TFRC did not prevent, but rather promoted CALR del52 induced proliferation of UT-7/Tpo CALR del52 but not UT-7/Tpo control cells[29] (**Supplementary Figure 5D**). Likewise, addition of recombinant exogeneous sTFRC, which retains immature glycans on Asn727 but not on Asn251[24], to culture medium did not prevent but increased activation of TpoR by CALR del52 in a rogue cytokine fashion (**Figure 5D**)

Next, we confirmed the activation of the JAK-STAT pathway by detection of phosphorylated STAT5, ERK1/2 and phosphorylated tyrosine 626 of the intracellular domain of TpoR [30], in BaF3 TpoR *Calr*^{mut} cells post-stimulation by 0.1µg/mL (C_p=7.3ng/mL) for several time points (**Figure 5E**). BaF3 parental cells did not show any such response up to 100µg/mL (C_p=7.3µg/mL) rhCALR del52 concentration (**Supplemental Figure 6A**). Finally, we harvested megakaryocytic (CD41$^+$) cells harboring a heterozygous *Calr* del52 mutation from the bone marrow of *Calr* $^{del52/WT}$ knock-in mice[14] (**Supplementary Figure 6B**) and subjected them to western blotting after stimulation for 30 min with rhCALR del52 or the vehicle control (**Supplementary Figure 6C**). Upon stimulation with 10µg/mL (C_p=730ng/mL) of rhCALR del52, we detected an increased phospho-STAT5 signal when compared to the vehicle condition, showing that exogenous CALR mutant proteins effectively activate the TpoR of primary *Calr*$^{del52/WT}$ cells.

Soluble CALR mutant proteins are able to directly interact with TpoR at the cell surface

In a previous study we provided evidence that when mutant CALR and TpoR are co-expressed in the same cell, a direct *cis* interaction can be documented either by Bioluminescence Resonance Energy Transfer (BRET) or by size-exclusion chromatography [12]. We used our previously published NanoBRET constructs [12] and set-up a cell co-culture system assay to assess *trans* interaction between cells stably expressing either CALR del52-HaloTag or NanoLuc-TpoR (NL-TpoR) (**Figure 6A**). Both construct types were properly expressed and/or secreted in the culture medium and recapitulated the signaling properties of the original protein (**Supplementary Figure 7**). By co-culture of these cells, we observed that CALR del52-HaloTag has a stronger interaction with NL-TpoR *in trans* than that of CALR WT-HaloTag (**Figure 6B**). To confirm this finding, we incubated BaF3 TpoR $CALR^{WT}$ or BaF3 TpoR $CALR^{mut}$ with rhCALR del52 for a short timeframe (15 minutes) and measured by western blotting the binding of exogeneous rhCALR del52 to these cells after extensive washing (**Figure 6C**). Strongest binding was observed on BaF3 TpoR $CALR^{mut}$ even at low physiological concentration (0.1µg/mL) *(***Figure 6D***)*. At higher concentration (0.5µg/mL), weak binding was also detected for BaF3 TpoR $CALR^{WT}$ cells (**Figure 6D**), in line with our functional assays showing that much higher levels of rhCALR del52 are required for activation of signaling in cells expressing TpoR and CALR WT but not the mutant CALR (**Supplementary Figure 5B**).

Recombinant CALR del52 is able to enhance the differentiation of human megakaryocyte progenitors *ex vivo*

Next, we sought to validate the cytokine effect of rhCALR del52 in primary cells from patients with MPN carrying *CALR* mutations, or *JAK2* V617F or healthy controls. We isolated $CD34^{+}CD41^{+}$ cells and performed megakaryocyte (MK) colony assays in the absence or presence of rhCALR del52 in medium containing KIT ligand (SCF) and lipids, insulin-transferrin and BSA. In this medium for colony assays, the half-life of rhCALR del52 is ~35 min (**Figure 7A**).

We first used a single dose of 20µg/mL (C_p=120ng/mL over 5 days) rhCALR del52 and observed that rhCALR del52 significantly increased the number of MK colonies, while CALR WT did not (**Figure 7B**). Importantly, rhCALR del52 did not increase the number of MK colonies for JAK2 V617F patients or for healthy controls (**Figure 7C-D**). Alternatively, we added a lower amount of rhCALR del52 daily to mimic *in vivo* conditions where CALR del52 is continuously produced and to partially compensate

the rapid disappearance of the recombinant protein. To this end we added daily for 4 days either 0.1µg/mL (C_p=3ng/mL); 1µg/mL (C_p=30ng/mL) or 5µg/mL (C_p=150ng/mL). We could detect a significant increase in Tpo-independent MK colonies in the condition of 5µg/mL (C_p=150ng/mL) of rhCALR del52, and a trend in the condition of 1µg/mL (C_p=30ng/mL) (**Figure 6E**). Taken together our data indicate that at levels comparable to the levels detected in patients, rhCALR del52 induces a significant increase in MK colony formation.

Discussion

Here we show that MPN patients that harbor *CALR* driver mutations exhibit plasma levels of mutant CALR proteins that correlate with the mutated *CALR* allele burdens. This finding raises the possibility of using the level of circulating CALR mutant proteins as a biomarker and risk-stratification of *CALR*-mutated MPNs. Indeed, the mean levels of circulating CALR mutants significantly differ between ET and (pre)-MF patients. Such secreted CALR mutant proteins can act as rogue cytokines to activate TpoR/JAK-STAT signaling in cell lines and patient primary cells. To our knowledge, this work is the first to demonstrate that circulating CALR mutant proteins can exert a 'rogue cytokine' activity on cells that express the TpoR. Cells that carry an oncogenic mutation of *CALR* are more sensitive to levels of exogenous CALR mutant proteins close to those detected in patient plasma. This can be explained as only cells expressing endogenous mutant CALR will expose at the cell-surface TpoR with immature (high mannose) N-glycosylation [12] required for binding to the lectin domain of CALR [31,32]. We propose a model where mutant CALR proteins are secreted from *CALR*-mutated cells, including cells from the clone that do not express TpoR, and can enhance the activation of the TpoR of a nearby *CALR*-mutated cell in a paracrine fashion. This model would apply notably to the bone marrow niche were levels can be higher than in plasma. While our work did not address the relative contribution of plasma versus intracellular CALR mutant for the expansion of the clone, our data indicates that plasma CALR mutant can act as an additional factor reinforcing the constitutive activation of TpoR mediated by intracellular CALR mutant [4-10].

The difference in half-lives between plasma CALR mutants and recombinant CALR mutant proteins in human plasma or culture medium indicate that upon secretion the mutant CALR proteins are in complexes with other proteins that stabilize them. We

identified sTFRC as a major partner that increases the half-life of CALR mutant proteins without preventing its rogue cytokine activity. Like TpoR, sTFRC retained immature N-glycans specifically in the presence of CALR mutant, indicating that the interaction occurs intracellularly and that the relevant complex is the one secreted by cells. The identification of this novel interaction comes together with recent observations that iron metabolism is dysregulated in CALR del52 expressing cells [33]. This suggests that this novel interaction may have broader effects on the MPNs pathology beyond the stabilization of plasma CALR mutant.

Recently, levels of secreted CALR (wild-type and mutant) were assessed in knock-in models [14,17,34] and MPN patient plasma [16] and are in agreement to ours. Remarkably, such secreted CALR exerted profound consequences on the immune response [16]. Our data suggest that removing the circulating CALR mutant proteins may give an effect on the phenotype of the MPN disease. In fact, an antibody targeting the CALR mutant when injected *in vivo* was able to detect and remove circulating mutant CALR and to reduce platelet numbers in a mouse model of MPN represented by KI of a chimeric murine-human CALR del52, where the tail of CALR del52 was from the human sequence [34].

Our finding that CALR mutant proteins act as rogue cytokines may open new perspectives for treating patients that are suffering from *CALR*-mutated MPNs.

Acknowledgements

We thank Dr. Didier Colau for protein production and purification and guidance with respect to recombinant protein usage, Lidvine Genet for expert technical support, and Dr. Nicolas Dauguet for flow cytometry assistance. AR was supported by de Duve Institute Morange Funds postdoctoral fellowship and by a FRS-FNRS fellowship. TB was supported by a PhD Télévie fellowship. SNC is Honorary Research Director at FRS-FNRS Belgium. NP has received an FSR PhD Fellowship from Université catholique de Louvain and an Aspirant PhD Fellowship from the FRS-FNRS, Belgium.

Funding to SNC is acknowledged from Ludwig Institute for Cancer Research, Fondation contre le cancer, Salus Sanguinis and Fondation “Les avions de Sébastien”, projets Action de recherché concertée (ARC) 16/21-073, Projet de recherche FNRS n°T.0043.21 and WelBio F 44/8/5 - MCF/UIG – 10955. The study was funded by grants from the Austrian Science Fund (P34451-B) and the Österreichische Forschungsförderungsgesellschaft (FFG) to RK. Studies conducted at the University of Pavia were supported by a grant from Associazione Italiana per la Ricerca sul Cancro (AIRC), MYNERVA project #21267 to MC.

The work of VW, IP, AT, MEK, CM was funded by the Ligue Nationale contre le Cancer (équipe labellisée 2019), INCA PLBIO 2016 and 2021 (IP), and from the INSERM. Labex GR-Ex (IP, WV) is funded by the program “Investissements d’avenir”. AT was supported by the university Paris-Diderot (MENRT grant) and then La ligue Nationale contre le cancer.

The work of TEF and DSM was supported by the Romanian Ministry of Education Research and Innovation, under grant number PN 19.29.01.02/2019.

Authorship contributions

CP, NP, TB, IC, AT planned paper strategy, performed experiments, interpreted data and wrote the paper; CP, AN, IC, GV, JPD planned and performed transcriptional experiments, CP performed functional murine cell lines and primary cell experiments, TB planned and performed BRET experiments, NP performed CALR mutant protein characterization from patient and primary mouse model plasmas, identify the TFRC-CALR interaction from plasma patients and performed characterization of the CALR-TFRC interaction, DV and NP performed mass spectrometry experiments and analyzed the data, EH , EX, OZ, RK performed study on patient plasma, EF and DSM performed immunoelectron microscopy, HG, BG, MS, IC, ER, DP, CC, LA, MC, NK, YK, YS, YE, MA, VBA, SH, VH selected patients, characterized allele burdens for MPN driver mutations and interpreted data on plasma levels of CALR mutants in the context of type of mutation, allele burden and MPN subtype. AT, MEK, CM performed megakaryocytic colonies from CALR-mutated patients and IP and VW supervised and analyzed these experiments. SNC, RK and WV planned research interpreted data and wrote the paper.

Conflict of Interest

RK and SNC and are co-founders of MyeloPro GmbH.

References

1. Nangalia J, Massie CE, Baxter EJ, et al. Somatic CALR Mutations in Myeloproliferative Neoplasms with Nonmutated JAK2. *N Engl J Med.* 2013;369(25):2391-2405.
2. Klampfl T, Gisslinger H, Harutyunyan AS, et al. Somatic Mutations of Calreticulin in Myeloproliferative Neoplasms. *N Engl J Med.* 2013;369(25):2379-2390.
3. Michalak M, Groenendyk J, Szabo E, Gold LI, Opas M. Calreticulin, a multi-process calcium-buffering chaperone of the endoplasmic reticulum. *Biochem J.* 2009;417(3):651-666.
4. Chachoua I, Pecquet C, El-Khoury M, et al. Thrombopoietin receptor activation by myeloproliferative neoplasm associated calreticulin mutants. *Blood.* 2016;127(10):1325-1335.
5. Nivarthi H, Chen D, Cleary C, et al. Thrombopoietin receptor is required for the oncogenic function of CALR mutants. *Leukemia.* 2016;30(8):1759-1763.

6. Elf S, Abdelfattah NS, Baral AJ, et al. Defining the requirements for the pathogenic interaction between mutant calreticulin and MPL in MPN. *Blood.* 2018;131(7):782-786.
7. Elf S, Abdelfattah NS, Chen E, et al. Mutant Calreticulin Requires Both Its Mutant C-terminus and the Thrombopoietin Receptor for Oncogenic Transformation. *Cancer Discov.* 2016;6(4):368-381.
8. Marty C, Pecquet C, Nivarthi H, et al. Calreticulin mutants in mice induce an MPL-dependent thrombocytosis with frequent progression to myelofibrosis. *Blood.* 2016;127(10):1317-1324.
9. Araki M, Yang Y, Masubuchi N, et al. Activation of the thrombopoietin receptor by mutant calreticulin in CALR-mutant myeloproliferative neoplasms. *Blood.* 2016;127(10):1307-1316.
10. Balligand T, Achouri Y, Pecquet C, et al. Pathologic activation of thrombopoietin receptor and JAK2-STAT5 pathway by frameshift mutants of mouse calreticulin. *Leukemia.* 2016;30(8):1775-1778.
11. Han L, Schubert C, Kohler J, et al. Calreticulin-mutant proteins induce megakaryocytic signaling to transform hematopoietic cells and undergo accelerated degradation and Golgi-mediated secretion. *J Hematol Oncol.* 2016;9(1):45.
12. Pecquet C, Chachoua I, Roy A, et al. Calreticulin mutants as oncogenic rogue chaperones for TpoR and traffic-defective pathogenic TpoR mutants. *Blood.* 2019;133(25):2669-2681.
13. Araki M, Yang Y, Imai M, et al. Homomultimerization of mutant calreticulin is a prerequisite for MPL binding and activation. *Leukemia.* 2018.
14. Balligand T, Achouri Y, Pecquet C, et al. Knock-in of murine Calr del52 induces essential thrombocythemia with slow-rising dominance in mice and reveals key role of Calr exon 9 in cardiac development. *Leukemia.* 2020;34(2):510-521.
15. Pecquet C, Balligand T, Chachoua I, et al. Secreted Mutant Calreticulins As Rogue Cytokines Trigger Thrombopoietin Receptor Activation Specifically in CALR Mutated Cells: Perspectives for MPN Therapy. *Blood.* 2018;132(Suppl 1):4.
16. Liu P, Zhao L, Loos F, et al. Immunosuppression by Mutated Calreticulin Released from Malignant Cells. *Mol Cell.* 2019.

17. Benlabiod C, Cacemiro MdC, Nédélec A, et al. Calreticulin del52 and ins5 knock-in mice recapitulate different myeloproliferative phenotypes observed in patients with MPN. *Nature Communications.* 2020;11(1):4886.
18. Dupuis M, Schaerer E, Krause KH, Tschopp J. The calcium-binding protein calreticulin is a major constituent of lytic granules in cytolytic T lymphocytes. *J Exp Med.* 1993;177(1):1.
19. Eggleton P, Lieu TS, Zappi EG, et al. Calreticulin Is Released from Activated Neutrophils and Binds to C1q and Mannan-Binding Protein. *Clinical Immunology and Immunopathology.* 1994;72(3):405-409.
20. Ogden CA, deCathelineau A, Hoffmann PR, et al. C1q and Mannose Binding Lectin Engagement of Cell Surface Calreticulin and Cd91 Initiates Macropinocytosis and Uptake of Apoptotic Cells. *J Exp Med.* 2001;194(6):781-796.
21. Gardai SJ, McPhillips KA, Frasch SC, et al. Cell-Surface Calreticulin Initiates Clearance of Viable or Apoptotic Cells through trans-Activation of LRP on the Phagocyte. *Cell.* 2005;123(2):321-334.
22. Feng M, Chen JY, Weissman-Tsukamoto R, et al. Macrophages eat cancer cells using their own calreticulin as a guide: Roles of TLR and Btk. *Proceedings of the National Academy of Sciences.* 2015;112(7):2145-2150.
23. Beguin Y. Soluble transferrin receptor for the evaluation of erythropoiesis and iron status. *Clinica Chimica Acta.* 2003;329(1):9-22.
24. Hayes GR, Williams A, Costello CE, Enns CA, Lucas JJ. The critical glycosylation site of human transferrin receptor contains a high-mannose oligosaccharide. *Glycobiology.* 1995;5(2):227-232.
25. Rowland M, Tozer TN. *Clinical pharmacokinetics/pharmacodynamics.* Lippincott Williams and Wilkins Philadelphia; 2005.
26. Thomas GR, Thibodeaux H, Errett CJ, et al. In Vivo Biological Effects of Various Forms of Thrombopoietin in a Murine Model of Transient Pancytopenia. *Stem Cells.* 1996;14(S1):246-255.
27. Zhao X, Feng X, Wu Z, et al. Persistent elevation of plasma thrombopoietin levels after treatment in severe aplastic anemia. *Exp Hematol.* 2018;58:39-43.
28. Wood TJ, Sliva D, Lobie PE, et al. Specificity of transcription enhancement via the STAT responsive element in the serine protease inhibitor 2.1 promoter. *Mol Cell Endocrinol.* 1997;130(1-2):69-81.

29. Wang S, He X, Wu Q, et al. Transferrin receptor 1-mediated iron uptake plays an essential role in hematopoiesis. *Haematologica.* 2020;105(8):2071-2082.
30. Drachman JG, Millett KM, Kaushansky K. Thrombopoietin signal transduction requires functional JAK2, not TYK2. *J Biol Chem.* 1999;274(19):13480-13484.
31. Michalak M, Corbett EF, Mesaeli N, Nakamura K, Opas M. Calreticulin: one protein, one gene, many functions. *Biochem J.* 1999;344 Pt 2:281-292.
32. Kapoor M, Ellgaard L, Gopalakrishnapai J, et al. Mutational analysis provides molecular insight into the carbohydrate-binding region of calreticulin: pivotal roles of tyrosine-109 and aspartate-135 in carbohydrate recognition. *Biochemistry.* 2004;43(1):97-106.
33. Greenbaum HS, Evers M, Rosencrance A, et al. Type I Calreticulin Mutations Result in Hyperactivation of Its Acetyltransferase Function and Iron Metabolism, Inducing a Susceptibility to Ferroptosis. *Blood.* 2021;138(Supplement 1):3593-3593.
34. Achyutuni S, Nivarthi H, Majoros A, et al. Hematopoietic expression of a chimeric murine-human CALR oncoprotein allows the assessment of anti-CALR antibody immunotherapies in vivo. *Am J Hematol.* 2021;96(6):698-707.

Figure legends

Figure 1:

Quantification of mutant-CALR in plasma MPN patients and correlation of their levels to the disease state.

(A) Quantification of free CALR mutant proteins in the plasma from MPN patients, separated by their mutational status, assayed by ELISA. Red bars represent mean ± Standard Deviation (SD). (B) Same ELISA results for *CALR*-mutated patients as shown in A, separated according to their mutation type. Red bars represent mean ± SD. **C.** XY plot of the allele burden of each patient by their level of free plasmatic mutant CALR. A linear regression was applied and shows a statistically significant correlation between the two parameters. **D.** Same ELISA results for *CALR*-mutated patients as shown in A, represented as a box and whisker plot, arranged according to their disease status. All statistical analysis (using the Prism6 software) were performed by the unpaired t-test.

Figure 2:

Immuno-electron microscopy of CALR.

(A) In BaF3 cells, Flag-tagged CALR-del52 localized in both the cis-Golgi (cG) and trans-Golgi (tG) compartments (blue arrows), as well as vesicles distributed between the trans-Golgi network and the plasma membrane (blue circles), suggesting it follows the secretory pathway to the cell surface. (B) By contrast, Flag-tagged CALR WT predominantly localized in the endoplasmic reticulum (ER) and nuclear heterochromatin (yellow arrows) and was less frequent in the Golgi network (cG, tG). (C) In cytokine-independent, proliferating CRISPR-modified BaF3 TpoR *Calr*^{mut} cells, which expressed both CALR-del52 as well as endogenous CALR, anti-N terminus

labeling was frequently observed at the plasma membrane (blue circles), suggesting CALR secretion is maintained in this cell line. (D) In control CRISPR BaF3 TpoR *Calr*^{wt} cells, endogenous CALR localized mostly in the nucleus (N), perinuclear space and endoplasmic reticulum (ER, yellow arrows) and the Golgi (G) network. (E) In primary *Calr* $^{del52/WT}$ KI mouse bone marrow cells, N-terminus labeled CALR could be detected within the Golgi network (not shown), as well as at the plasma membrane (blue circles), suggesting secretion of CALR is maintained in these cells. (F) In control *Calr* $^{WT/WT}$ mouse bone marrow cells, endogenous CALR was mostly localized at the endoplasmic reticulum (ER) and the nucleus (N). (G) When using a mutant-specific anti-CALR antibody labeling could be detected in the Golgi network of CRISPR-modified BaF3 TpoR *Calr*^{mut} cells (G, blue arrows), but also at the plasma membrane (H), including associated with ectosomes (blue circles). (I) Similarly, the mutant specific antibody identified CALR del52 in the secretory pathway of *Calr* $^{del52/WT}$ KI mouse bone marrow cells (blue arrows and circles). Gold particle size is on average 0.8 nm in (A) and 6 or 10 nm in (B-I). m– mitochondria.

Figure 3:

Secretion and stability of plasma CALR del52 in Calr del52/WT KI mouse and human MPN patients.

(A) Immunoprecipitation of murine plasma CALR del52 and Whole blood lysates. Secretion rate of CALR del52 was evaluated by comparing the cellular and plasmatic CALR del52 levels from blood of KI-*Calr* $^{del52/wt}$ mice expressing or not TpoR.

(B) Stability study of CALR mutant in plasma from MPN patients harboring CALR del52 mutant. Eight samples from MPN patients harboring CALR del52 mutant maintained at 37°C for various time points were measured in duplicate by ELISA and analyzed using a one-phase decay model (Prism6) to determine the averaged half-life (t1/2) and the Coefficient of determination (R2). Error bars represent standard deviations.

(C) Stability study of rhCALR del52 in culture medium in absence of FBS. A fixed amount of rhCALR del52 was incubated in culture medium at 37°C for various time before measurement by ELISA analysis using a one-phase decay model (Prism6) to determine the averaged half-life and R2. Errors bars represent standard deviations.

(D) CALR mutant proteins after immunoprecipitation in various MPN patients (left) and CALR mutant proteins of the same patients detected by ELISA (right).

Figure 4

Plasma soluble Transferrin Receptor 1 is a carrier protein for CALR mutant

(A) Allele burden and mutation profile of patients included in this study the analysis.

(B) Identification of partners of plasmatic CALR mutant. Plasma from 5 CALR mutant positive patients and 5 healthy control was isolated by immunoprecipitation with biotinylated anti-mutant CALR antibody. Immunoblot shows the presence of CALR mutant in the immunoprecipitation (IP) product detected with a different anti-mutant CALR antibody. The IP product was analyzed by non-targeted mass spectrometry to identify interacting partners.

(C) Truncated Violin plot of relative sTFRC amount found co-immunoprecipitating with plasma CALR del52. Negative control corresponds to the IP product after anti-CALR mutant immunoprecipitation to control for non-specific binding to anti-CALR mutant antibody.

(D) Stability study of rhCALR del52 in medium with 10% FBS, with or without addition of 2µg/mL or 4µg/mL of rhTFRC. rhCALR del52 mutant in different media was maintained at 37°C for various time points and measured by ELISA before analysis using a one-phase decay model (Prism6) to determine the averaged half-life (t1/2). Values represent mean of triplicate (+SD).

(E) Representative confocal microscopy pictures of HEK293T co-transfected with either CALR WT or CALR del52 fused to GFP at their C-terminus and TFRC fused to mCherry at its C-terminus. Microscopy analysis shows co-localization between CALR del52 and TFRC in subcellular compartments with high correlation between the two constructs.

(F) Immunoprecipitation and glycosylation profile analysis of endogenous TFRC from UT-7/Tpo or UT-7/Tpo CRISPR CALR del52. Western blot shows the TFRC forms analyzed by mass spectrometry. Data represents the percentage of Peptide-spectrum match (PSM) of immature N-glycans (high-mannose) present on residue Asn251 in the cleaved or full form of TFRC.

Figure 5

Exogenous CALR del52 is inducing cell growth and JAK/STAT signaling in BaF3 expressing TpoR and mutant CALR.

(A) Short term proliferation of parental BaF3 and stable BaF3 expressing the indicated constructs were analyzed after daily exposition of the indicated doses of rhCALR del52 during 72h with CTG assay (Promega). Values shown represent the average of 5 experiments with at least 29 biological replicates ± SEM.

(B) Short term proliferation of BaF3 TpoR CALR^{mut} were analyzed after daily exposition of 1µg/mL of rhCALR del52, 0.1ng/mL of Tpo or 10ng/mL of Tpo during 72h with CTG assay (Promegq). Average ± SD of 6 replicates. (A-B). Statistical analysis (Jmp pro14) was performed by the non-parametric multiple comparisons Steel's test with a control group (vehicle). ****, $p < 0.0001$, *** $=p < 0.001$, ** $=p < 0.01$, ns: non-significant.

(C) BaF3 TpoR *Calr*^{mut} cells were transiently transfected with the Spi-Luc luciferase STAT5 reporter and the internal control pRL-TK used for normalization. The cells were cultured with different concentrations of recombinant human CALR del52 or CALR WT during 24h before performing a dual-luciferase assay for STAT5 transcriptional activity.

(D) BaF3 TpoR *Calr*^{mut} cells transfected with Spi-Luc and pRL-TK were treated during 24 h with vehicle, 1µg/mL of rhCALR del52 and indicated molar rations of rhTFRC and STAT5 transcriptional activity was measured by Dual Luciferase assay (Promega). (C-D) Luciferase activity is normalized to vehicle condition (⌀). Values shown represent the average of 6 to 12 biological replicates ± SEM. Statistical analysis (Jmp pro14) was performed by the non-parametric multiple comparisons Steel's test with a control group (⌀). *** $=p < 0.001$, ** $=p < 0.01$, * $=p < 0.05$. Statistical analysis of two specific conditions (see dashed lines) were performed by the unpaired t-test.

(E) Western blots showing time-dependent phosphorylation of TpoR, STAT5 and ERK1/2 in BaF3 TpoR *Calr*^{mut} treated or not with 0.1µg/mL of rhCALR del52 for various times (5, 10, 15, 30, 45, 60 min). P-Y626-TpoR denotes phosphorylation of tyrosine residue 112 of the intracellular chain of TpoR. HA denotes detection of total HA-tagged TpoR.

Figure 6:

Binding of soluble CALR mutant proteins to TpoR at the cell surface

(A) Cartoon representation of our exogenous CALR, co-cell culture NanoBRET setup. H: Halo-Tag, fused to the C-term of CALR. NL: Nano-luciferase, fused to the N-term of TpoR. 618-ligand: fluorescent molecule with very high affinity for HaloTag. The circle represents a BRET phenomenon that occurs only when the energy donor (NL) is within 10 nm of the energy acceptor (618-ligand).

(B) BRET detection between CALR-HaloTag and cell-surface Nano-luciferase-TpoR in a stable cell co-culture assay. HEK293 cells stably expressing either CALR WT or del52-HaloTag were co-cultivated overnight in presence of 618-ligand with HEK293 cells stably expressing NL-TpoR. Data from 3 independent experiments were pooled and values were normalized to the NL-TpoR & CALR WT-Halo condition. Statistical analysis (Jmp pro14) was performed by a two-tailed student's t-test and *p*-value is shown above.

(C) Cartoon representation of our assay to measure binding of rhCALR del52 to BaF3 TpoR *Calr*^{wt} and BaF3 TpoR *Calr*^{mut}. Cells were incubated for 15 minutes with varying amount of rhCALR del52 prior to extensive washing.

(D) Western blotting showing the presence of rhCALR del52 bound to BaF3 TpoR *Calr*^{wt} and BaF3 TpoR *Calr*^{mut} after 15 minutes incubation with different concentration of rhCALR del52.

Figure 7: Induction of differentiation of megakaryocyte progenitors by CALR del52

(A) Stability study of recombinant human CALR del52 CFU-MK culture medium. Six samples maintained at 37°C for various time points were measured in duplicate by ELISA and analyzed using a one-phase decay model (Prism6) to determine the averaged half-life (t1/2) and the Coefficient of determination (R2). Error bars represent standard deviations.

CD34+CD41+ progenitors from four to six CALR-mutated patients (B), three JAK2 V617F patients (B) and three normal controls (C) were sorted and cloned at 1 cell/well in 96 well plates in serum-free medium containing SCF and treated with a single dose large dose of CALR del52. Percentages of MK colonies were calculated compared to the Tpo condition. Results are shown as mean ± SEM. **** =p < 0.0001, *** =p < 0.001. (one-way ANOVA, Holm-Sidak's multiple comparisons test).

(D) Effect of daily treatment of CALR del52 (0.1, 1, 5µg/mL) on MK colonies formation. CD34+CD41+ progenitors from four CALR-mutated patients were tested

and the percentages of MK colonies were calculated compared to the Tpo condition. Results are shown as mean ± SEM. ** represents significant difference $p<0.01$ (one-way ANOVA, Holm-Sidak's multiple comparisons test).

Figure 1

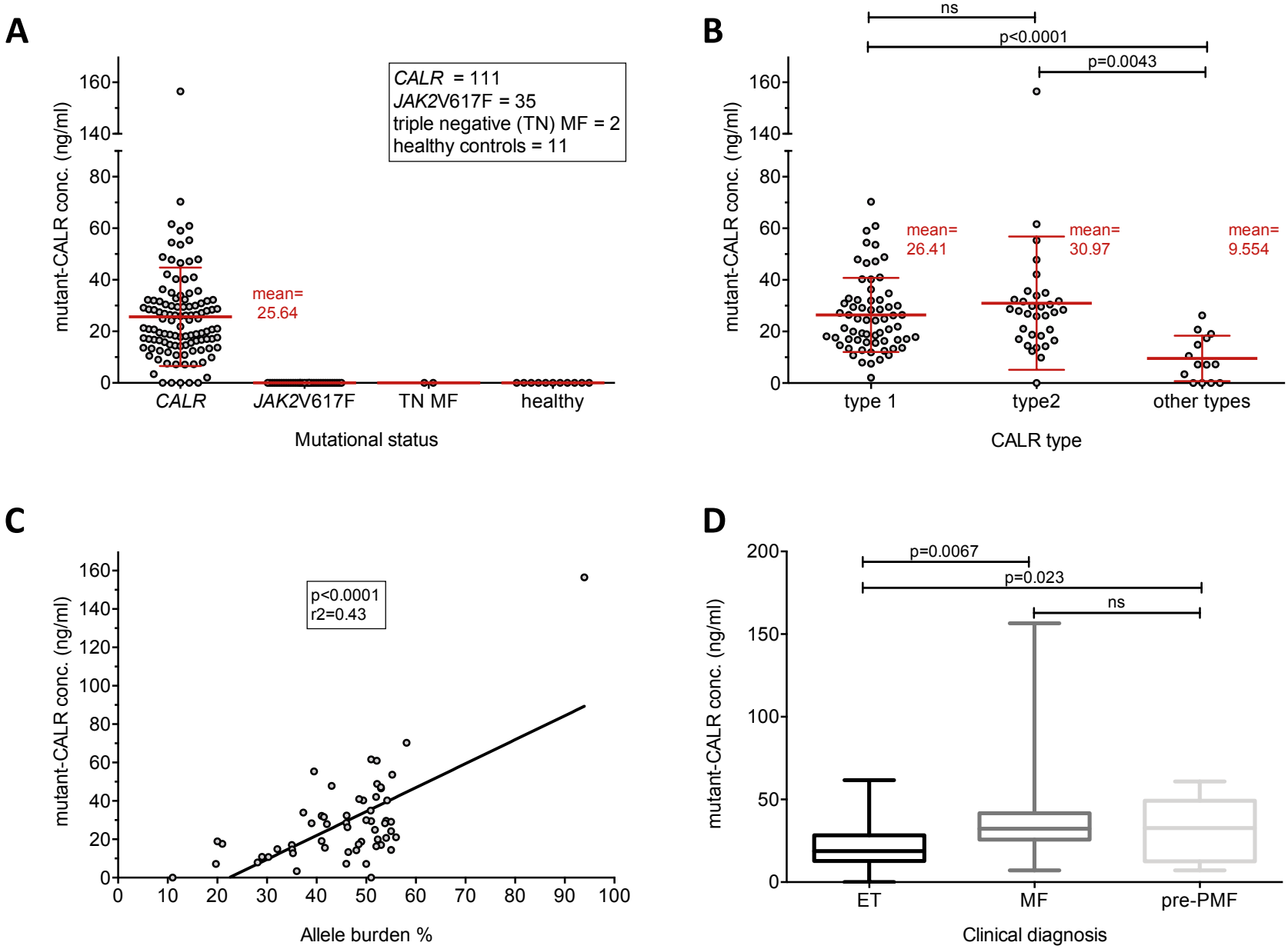
A
CALR = 111
JAK2V617F = 35
triple negative (TN) MF = 2
healthy controls = 11
mean= 25.64
mutant-CALR conc. (ng/ml)
CALR
JAK2V617F
TN MF
healthy
Mutational status
B
ns
p<0.0001
p=0.0043
mean= 26.41
mean= 30.97
mean= 9.554
type 1
type2
other types
CALR type
C
p<0.0001
r2=0.43
Allele burden %
D
p=0.0067
p=0.023
ns
ET
MF
pre-PMF
Clinical diagnosis

Figure 2

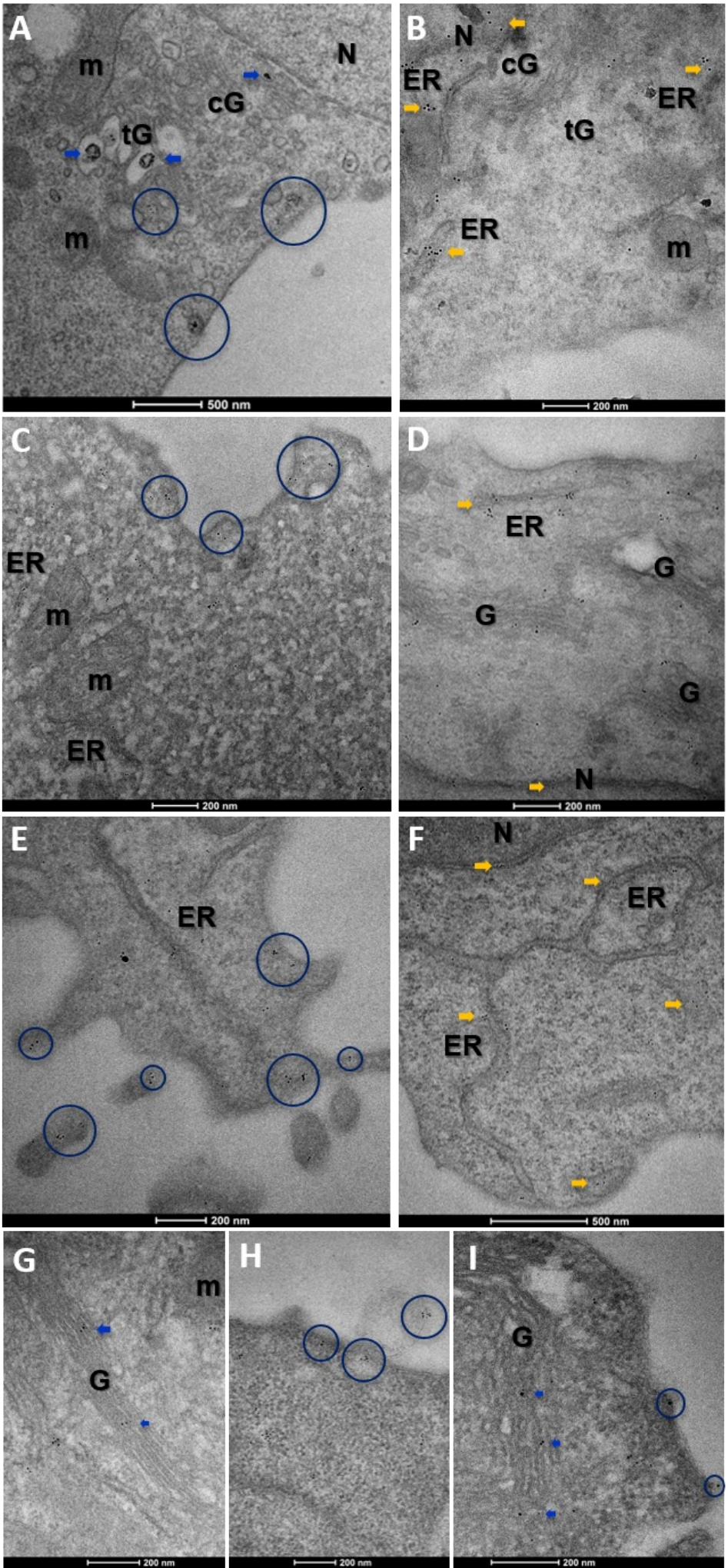
A
m
N
cG
tG
m
500 nm
B
N
cG
ER
ER
tG
ER
m
200 nm
C
ER
m
m
ER
200 nm
D
ER
G
G
G
N
200 nm
E
ER
200 nm
F
N
ER
ER
500 nm
G
m
G
200 nm
H
200 nm
I
G
200 nm

Figure 3

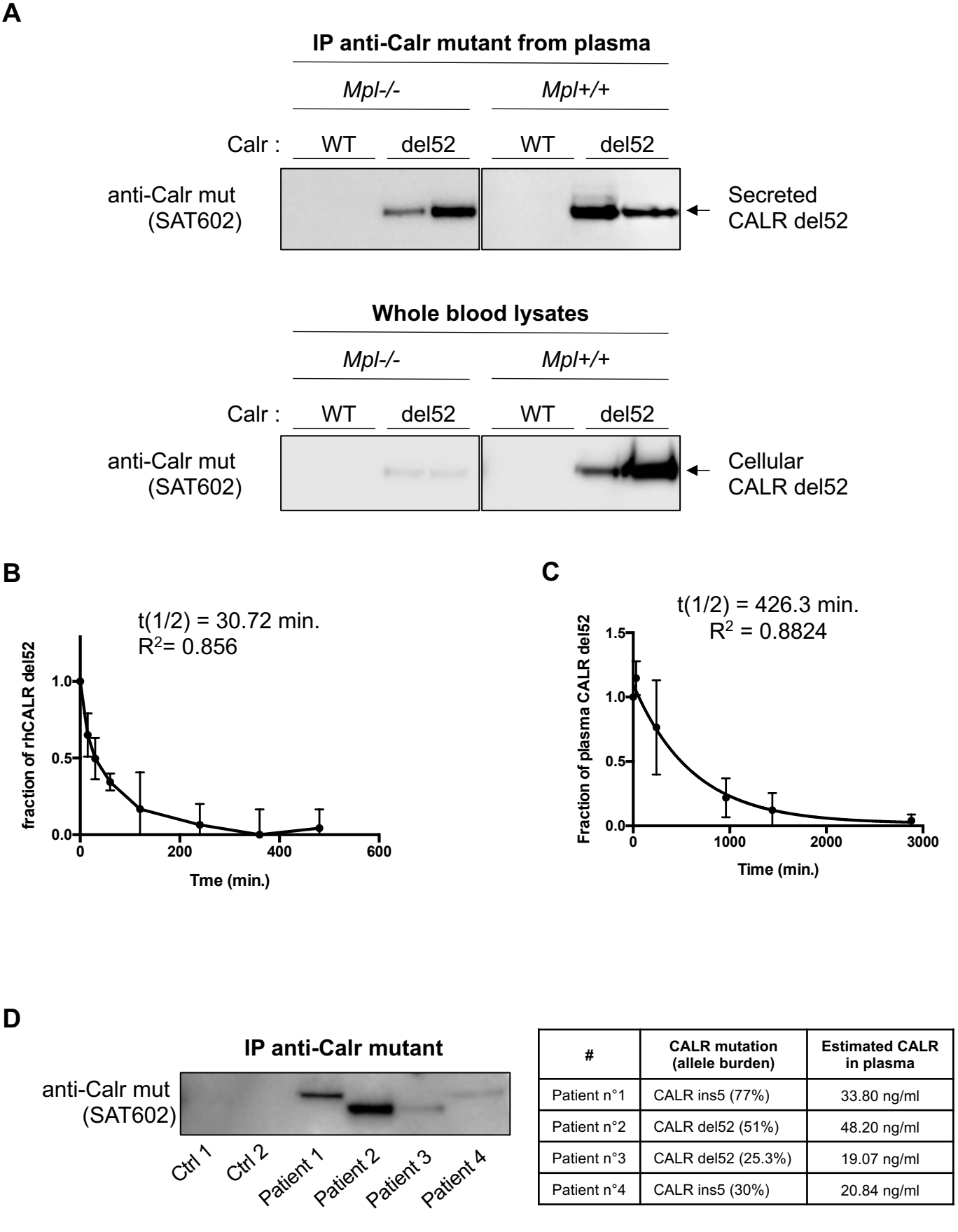

#	CALR mutation (allele burden)	Estimated CALR in plasma
Patient n°1	CALR ins5 (77%)	33.80 ng/ml
Patient n°2	CALR del52 (51%)	48.20 ng/ml
Patient n°3	CALR del52 (25.3%)	19.07 ng/ml
Patient n°4	CALR ins5 (30%)	20.84 ng/ml

Figure 4

A

	Allele burden	CALR mutation type
Patient 1	51%	Type 1
Patient 2	30%	Other
Patient 3	48%	Type 1
Patient 4	77%	Type 2
Patient 5	22.8%	Type 1

B

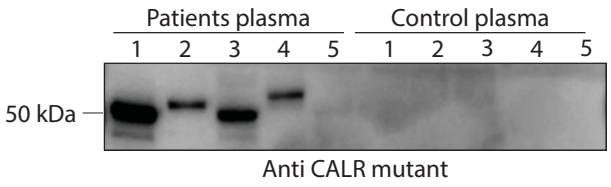

C

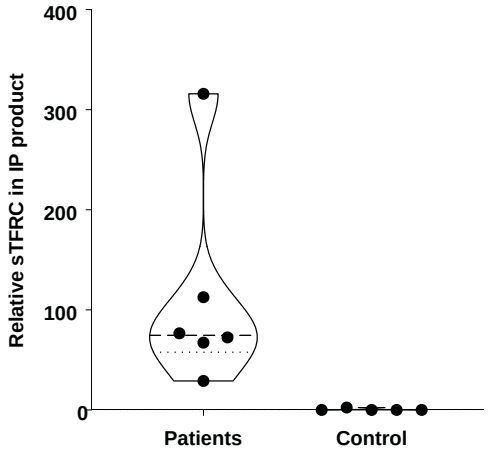

D

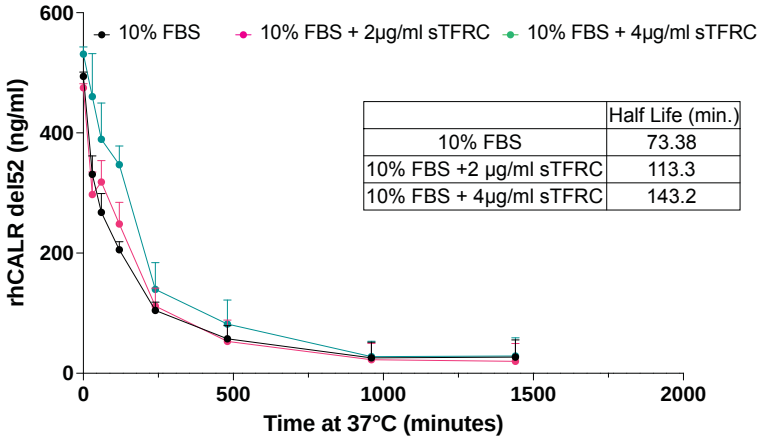

	Half Life (min.)
10% FBS	73.38
10% FBS +2 µg/ml sTFRC	113.3
10% FBS + 4µg/ml sTFRC	143.2

E

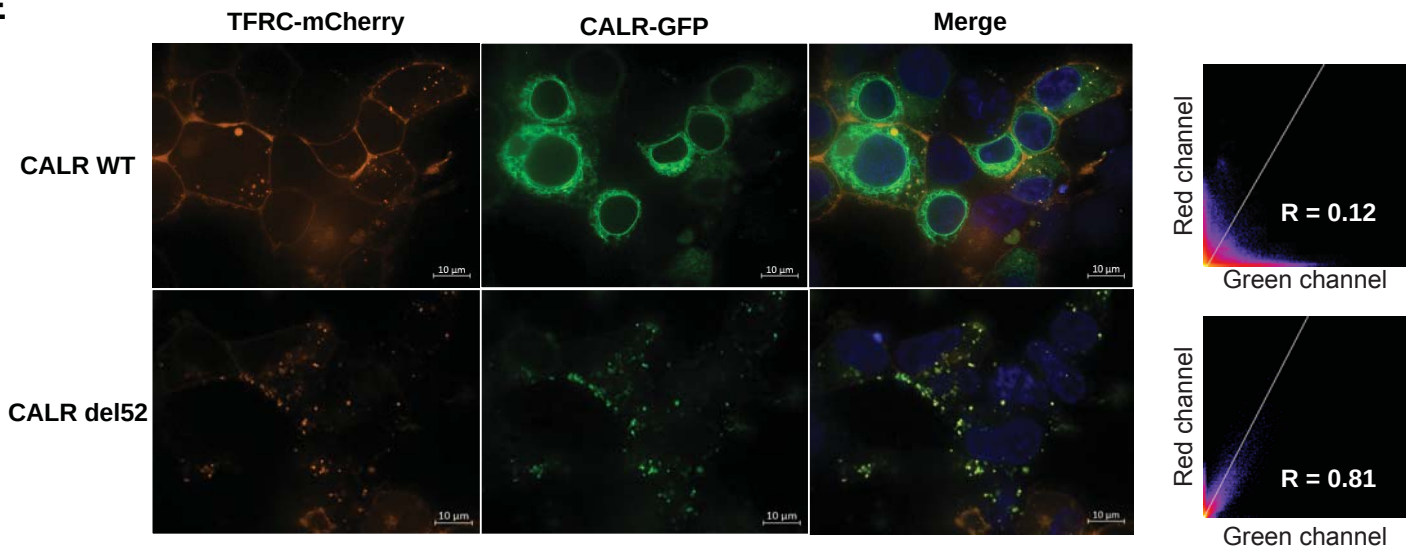

F

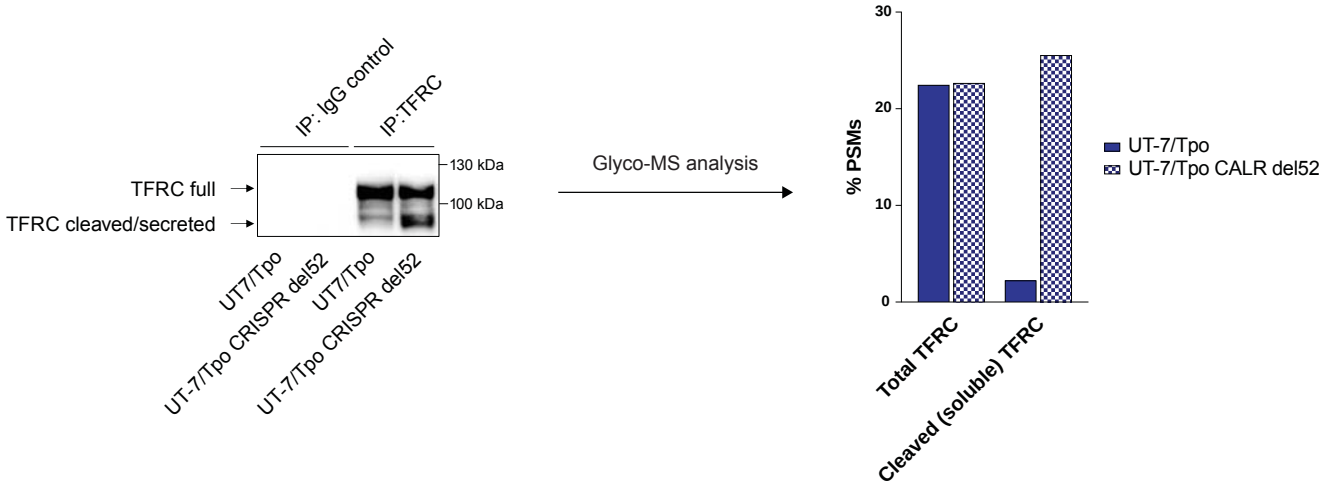

Figure 5

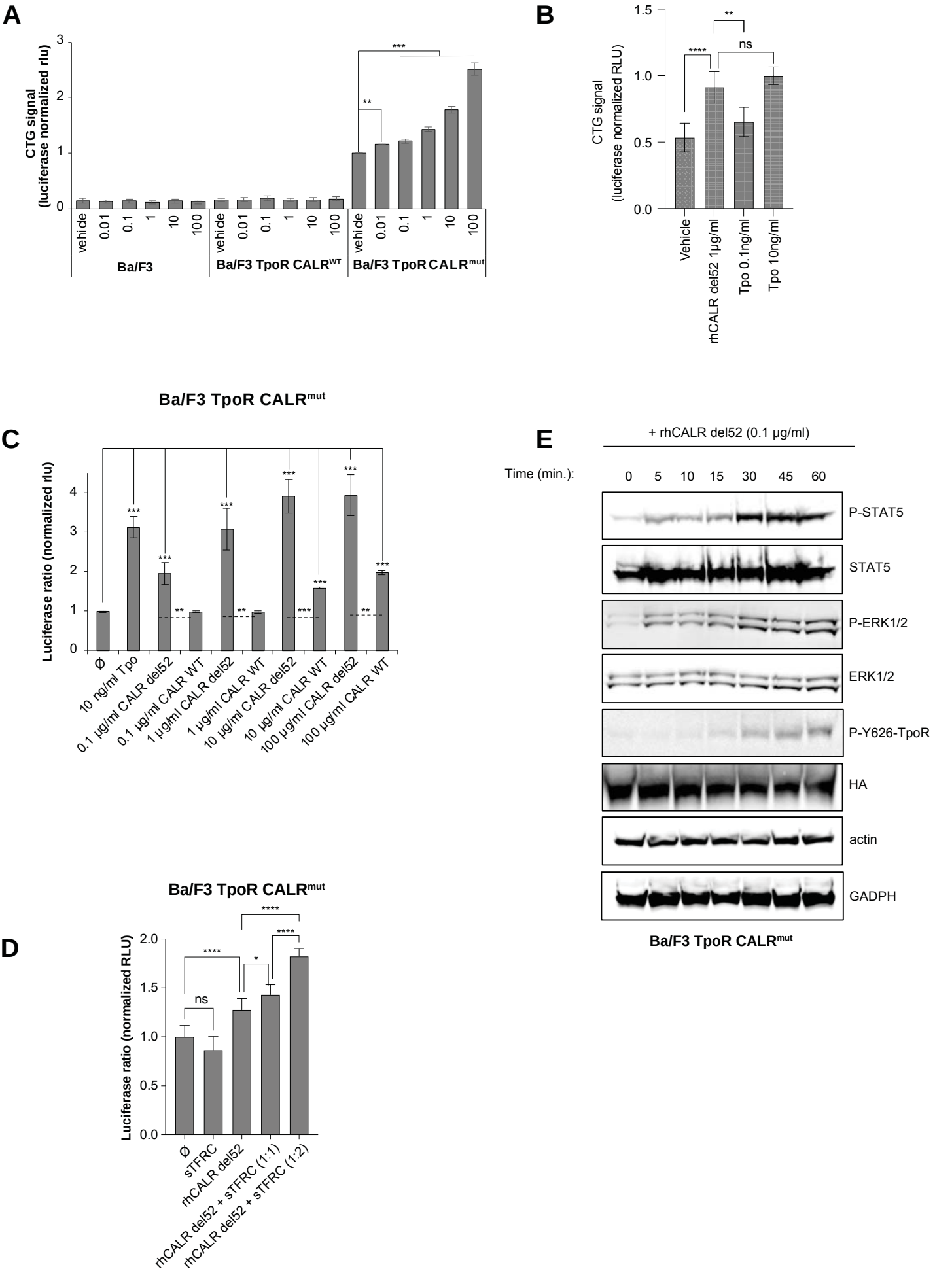
A
CTG signal (luciferase normalized rlu)
vehicle
0.01
0.1
1
10
100
Ba/F3
Ba/F3 TpoR CALR^WT
Ba/F3 TpoR CALR^mut
B
CTG signal (luciferase normalized RLU)
Vehicle
rhCALR del52 1µg/ml
Tpo 0.1ng/ml
Tpo 10ng/ml
ns
Ba/F3 TpoR CALR^mut
C
Luciferase ratio (normalized rlu)
Ø
10 ng/ml Tpo
0.1 µg/ml CALR del52
0.1 µg/ml CALR WT
1 µg/ml CALR del52
1 µg/ml CALR WT
10 µg/ml CALR del52
10 µg/ml CALR WT
100 µg/ml CALR del52
100 µg/ml CALR WT
D
Ba/F3 TpoR CALR^mut
Luciferase ratio (normalized RLU)
Ø
sTFRC
rhCALR del52
rhCALR del52 + sTFRC (1:1)
rhCALR del52 + sTFRC (1:2)
ns
E
+ rhCALR del52 (0.1 µg/ml)
Time (min.):
0
5
10
15
30
45
60
P-STAT5
STAT5
P-ERK1/2
ERK1/2
P-Y626-TpoR
HA
actin
GADPH
Ba/F3 TpoR CALR^mut

Figure 6

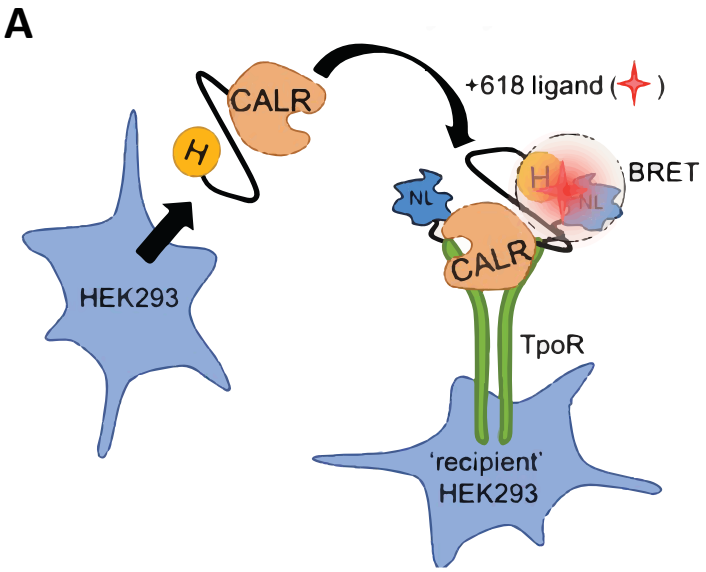
A
CALR
H
+618 ligand (✦)
BRET
H
NL
NL
CALR
HEK293
TpoR
'recipient'
HEK293

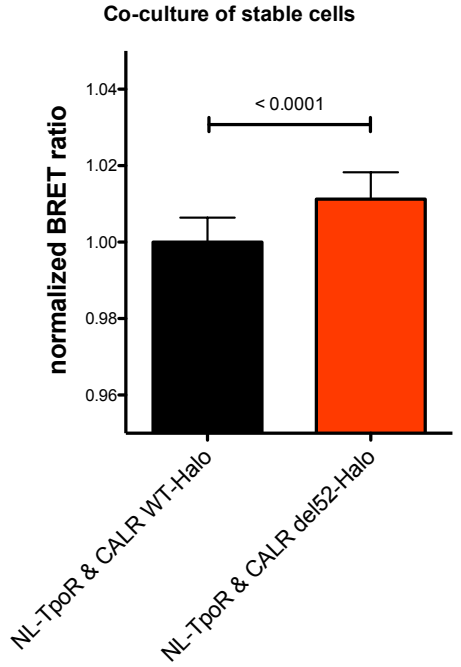
B
Co-culture of stable cells
normalized BRET ratio
1.04
1.02
1.00
0.98
0.96
< 0.0001
NL-TpoR & CALR WT-Halo
NL-TpoR & CALR del52-Halo

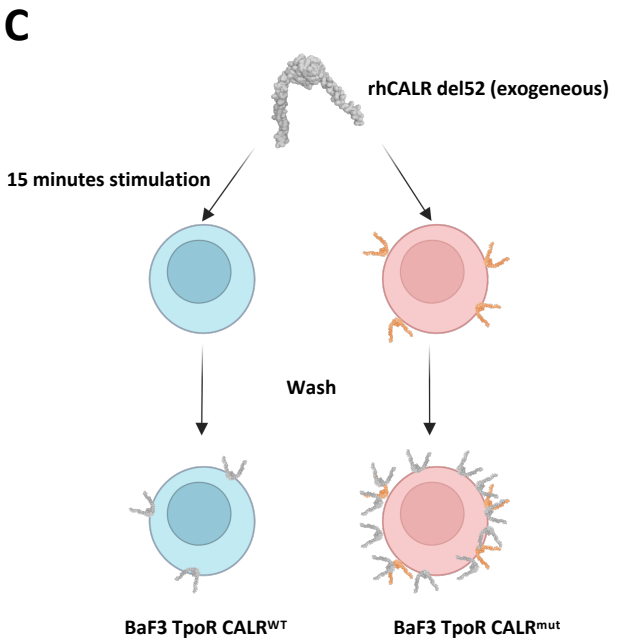
C
rhCALR del52 (exogeneous)
15 minutes stimulation
Wash
BaF3 TpoR CALRWT
BaF3 TpoR CALRmut

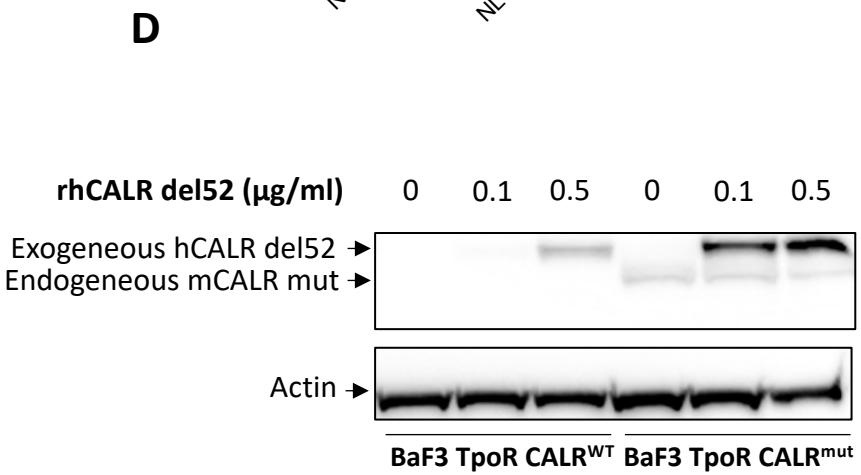
D
rhCALR del52 (µg/ml)
0
0.1
0.5
0
0.1
0.5
Exogeneous hCALR del52
Endogeneous mCALR mut
Actin
BaF3 TpoR CALRWT
BaF3 TpoR CALRmut

Figure 7

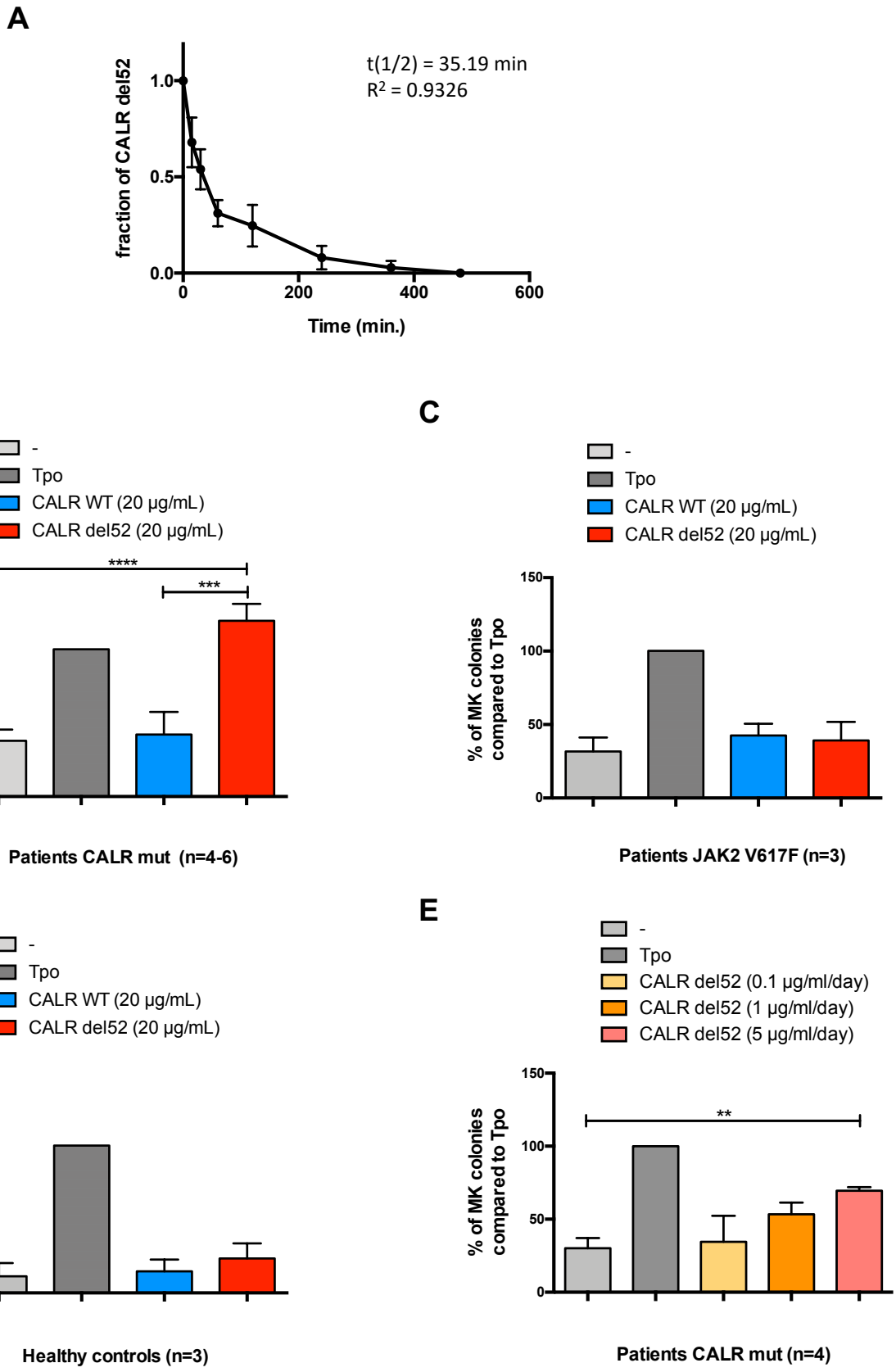
A
t(1/2) = 35.19 min
R2 = 0.9326
fraction of CALR del52
1.0
0.5
0.0
0
200
400
600
Time (min.)
B
-
Tpo
CALR WT (20 µg/mL)
CALR del52 (20 µg/mL)
****
***
% of MK colonies compared to Tpo
150
100
50
0
Patients CALR mut (n=4-6)
C
-
Tpo
CALR WT (20 µg/mL)
CALR del52 (20 µg/mL)
% of MK colonies compared to Tpo
150
100
50
0
Patients JAK2 V617F (n=3)
D
-
Tpo
CALR WT (20 µg/mL)
CALR del52 (20 µg/mL)
% of MK colonies compared to Tpo
150
100
50
0
Healthy controls (n=3)
E
-
Tpo
CALR del52 (0.1 µg/ml/day)
CALR del52 (1 µg/ml/day)
CALR del52 (5 µg/ml/day)
**
% of MK colonies compared to Tpo
150
100
50
0
Patients CALR mut (n=4)